Penerbit Akademia Baru

CFD Letters

Journal homepage: www.akademiabaru.com/cfdl.html
ISSN: 2180-1363

Alternative Design of Air Ventilation in Passenger Lift for Thermal Comfort

Open Access

Tristan Yeo Eng Kee[1], Chong Kok Hing[1,*], Basil Wong Tong Liong[1], Victor Bong Nee Shin[1], Lee Man Djun[2], Christopher Jantai Anak Boniface[3]

[1] Department of Mechanical Engineering, Faculty of Engineering, Computing and Science, Swinburne University of Technology Sarawak Campus, Jalan Simpang Tiga, 93300 Kuching, Sarawak, Malaysia
[2] School of Engineering and Technology, University College of Technology, 96000 Sibu, Sarawak, Malaysia
[3] Public Works of Department, Wisma Saberkas Building, Tun Abang Haji Openg Road, 93582, Kuching, Sarawak, Malaysia

ARTICLE INFO

Article history:
Received 21 November 2019
Received in revised form 16 January 2020
Accepted 21 January 2020
Available online 29 January 2020

ABSTRACT

Thermal comfort is an important aspect for passenger lift operation. It is a common experience to encounter thermal discomfort, especially in crowded passenger lifts. The interior temperature of passenger lifts is the deciding factor of thermal comfort, which is dependable on the size of the lift, number of passengers, air vents size and ventilation system. This study investigated an alternative design by replaced the intake fan with an exhaust fan and by introduced automatically operated dynamic air vents. This concept of integrated an exhaust fan and dynamic air vents is conducted on a Schindler passenger lift with FLUENT. The simulations conducted are compared with the conventional design, where airflow pattern, airflow velocity, and temperature changes are studied. Airflow analysis showed that the alternative ventilation system promoted a well-distributed airflow pattern within the lift with an average air velocity of 0.5 m/s at specific dynamic air vent angles. The air temperature surrounding the passenger is cooled and maintained at an average 24 °C while maintaining the overall interior temperature. The temperature difference between the human head and the lower body region for the conventional and alternative system were 3 °C and 2 °C, respectively. The airflow pattern, airflow velocity, and temperature changes with the alternative design are observed to be better than those of the conventional design. Hence, the proposed design offers an alternative to improve thermal comfort inside passenger lift.

Keywords:
Thermal comfort; temperature; numerical modelling; elevator; air vent

1. Introduction

Technological advances have led to the ability of passenger elevators being to reach greater heights and speeds to accommodate the ever-increasing number of high-rise buildings. Most modern passenger elevators are located at the centre of the building for the convenience of the users in the building, which meant that the lift shafts would require proper ventilation to ensure passenger comfort. Some designs incorporated high power exhaust fans on top of the lift shafts whereas others rely on small units of intake fans on top of the lifts. These are reasonable in terms of properly

* *Corresponding author.*
E-mail address: kchong@swinburne.edu.my (Chong Kok Hing)

ventilating air but may not effectively promoting passenger thermal comfort. Thus, some designs implement air conditioning to improve passenger thermal comfort at the expense of increasing electrical energy.

Elevator designers heavily emphasize on safe, user-friendly, and environment-friendly designs, which are paramount [1]. Conversely, most designs lack the thermal comfort consideration as passengers only use lifts for short periods to travel between floors. Many research studies were conducted to improve the elevators' user and environmental-friendliness, such as the following: Zhang *et al.,* [2] developed elevator ride comfort test with smartphone to enable economical measurement; development elevator monitoring system with Internet of Things to monitor elevator fault diagnosis and maintenance purposes [3]; sensor data driven elevator scheduling to achieving delivery and energy efficiently [4]; utilized induced airflow for kinetic energy harvesting in electricity generation [5]. Moreover, Al-Sharif and Hammoudeh developed a two-dimensional elevator traffic system to deliver effective traffic time usage [6]. In the area of safety, Yang, Kim and Lee developed a coupled vibration analysis theoretical model for building and elevator rope [7]. Kwon *et al.,* [8] evaluated the flexural and fatigue conditions of elevator carbon fibre reinforced plastic rope with various epoxy resin formulation. Multi-sensors employment were used to determine the torsion angles of the elevator guide rail for safety purpose [9].

Based on the literature review, it is clear that many research conducted on passenger lift safety, user-friendly, and environment-friendly aspects; however, there is little or no research on the passenger thermal comfort. This knowledge gap can benefit passenger lift industry to design cabin that provide passenger thermal comfort. In this study, the thermal comfort of passenger will be studied to fill in the identified knowledge gap. Thermal comfort is subjective and difficult to measure, but temperature, airflow velocity, and relative humidity can be controlled and measured [10]. These three controlling measures, especially interior temperature and airflow velocity are considered when gathering the simulation results from both conventional and alternative air ventilation designs. In addition, the study analyses the optimal dynamic air vent angle to promote optimal airflow into the lift, which aids in the efficiency of exhaust fan in performing air exchanges.

2. Methodology

2.1 Geometric Model

In this study, Solidworks software is utilized to model both conventional and alternative air ventilation designs that are based on the Schindler 5500 MRL elevator with interior car dimensions (width, depth and height) of 2100 mm, 1400 mm, and 2400 mm, respectively. The passenger lift is assumed to be travelling at the constant speed of 1.0 m/s during the simulation. Two distinct geometries of the passenger lift were prepared, where one has the conventional ventilation design consisting of a cross-flow intake fan and ventilation holes (Figure 1), and the other is of the proposed alternative design with an exhaust fan and dynamic air vents (Figure 2). Seventeen (17) geometries of the proposed ventilation design were prepared, each with differing dynamic vent dampers' angle at an increment of 10° to determine the optimal damper angle for the desired airflow velocity. A damper angle of 0° indicates that the dampers are perpendicular with respect to the lift walls and are simulated up to a maximum angle of 80° in both rotational directions shown in Figure 3.

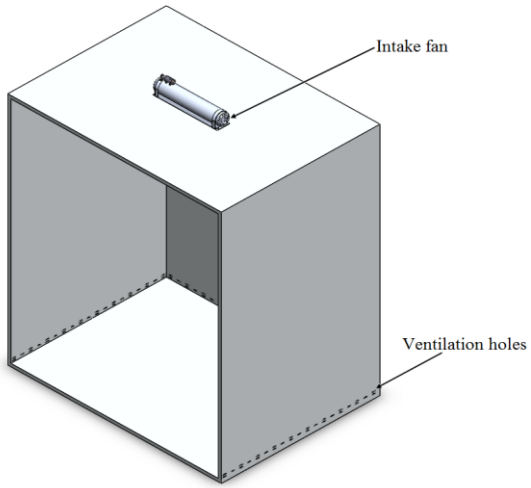

Fig. 1. Conventional ventilation system

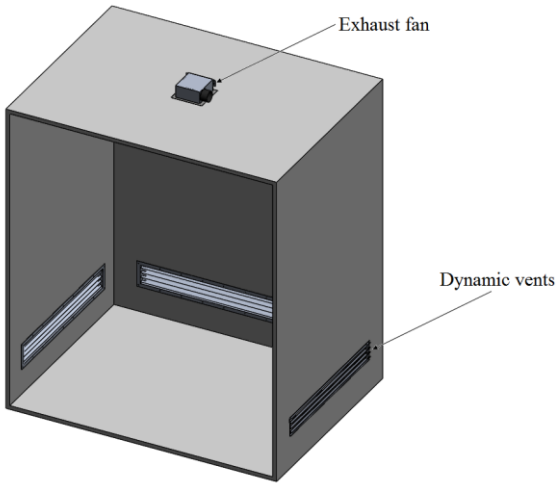

Fig. 2. Alternative ventilation system

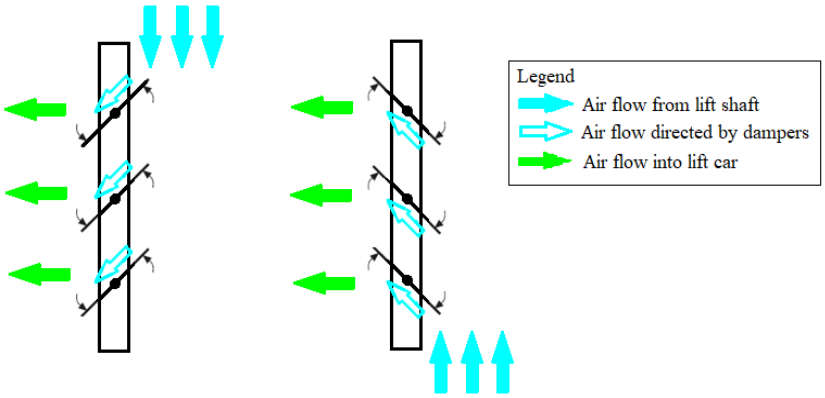

Fig. 3. Air flow into passenger lift when travelling upwards (left) and downwards (right)

The geometry of the human model was simplified and prepared, based on available data on the 50th percentile anthropometric data of a 40-year-old male [11]. The model consisted of four main sections: the head, the chest, the arms, and the legs. Temperature and velocity readings will be recorded at 15 mm to 20 mm above the surface of the human body for both systems to compare the simulations' results. The ventilation system for both conventional and alternative designs will consist of inlets and outlets, where the conventional system has one inlet and three main outlet sections, and the alternative system has three inlets and one outlet.

The conventional ventilation design is an intake fan that blows air into the lift from the top and ventilation holes located at the lower side walls. The proposed ventilation system consists of an exhaust fan located at the centre of the lift roof and dynamic air vents located at the lower sides and rear walls of the lift. The concept of implementing dynamic air vents is to allow optimal airflow rate into the lift car without the need to increase the exhaust fan's power supply. In this study, the dynamic air vents are designed with horizontal vanes, or dampers, which can rotate automatically using an actuator depending on the lift's direction of travel. The function of the dynamic air vents is to direct air flowing past the outside walls into the lift, which is further aided by the negative pressure formed within the lift due to the exhaust fan. These two components work in tandem to allow air to flow into the lower section of the lift to the upper section to be expelled, bringing odour and heat generated from the occupants along with it. Limaye *et al.,* [10] states that airflow directivity is affected by the orientation, number, shape and position of the air vents within a cabin.

In this study, the airflow directivity within the lift is determined by the dynamic air vents and the direction of lift travel. When the lift is travelling upwards, airflow from the top to the bottom of the lift exterior. The dynamic air vents will automatically rotate the dampers into the direction of the travel to introduce the airflow and direct it into the lift as shown in Figure 1. The optimal angle is determined with FLUENT 18.2 computational fluid dynamics. The intake cross flow fan (Model: JE-060A) for the conventional system and exhaust fan (Model: T050) is selected [12,13]. The selected model has similar operating specifications for passenger lifts installation.

The geometric models prepared on Dassault Systèmes SolidWorks are imported to ANSYS Fluent for meshing, setup, simulation, and analysis of results. This study used ANSYS 18.2 Fluent Fluid Flow and DesignModeler systems. SpaceClaim Computer-Aided Design (CAD) software is used as part of ANSYS 18.2 to prepare and convert the geometries into ANSYS-friendly documents. Using this software, a fluid volume of the passenger lift interior is created and documented. The geometries are meshed using ANSYS Mesh. Due to the education version (ANSYS) imposed, each meshed model consisted of no more than 512,000 tetrahedral cells with average skewness of 0.23. A high mesh quality with a minimum mesh size of 1 mm is created just around the inlets, outlets, and human models to obtain more accurate airflow characteristics. The air vents' dampers are 2 mm thick so the mesh size of 1mm is defined to accurately capture the geometry. Moreover, this mesh size allows accurate capture of the human model. Figure 4 shows the meshed fluid volume of the passenger lift with the alternative ventilation system and human model.

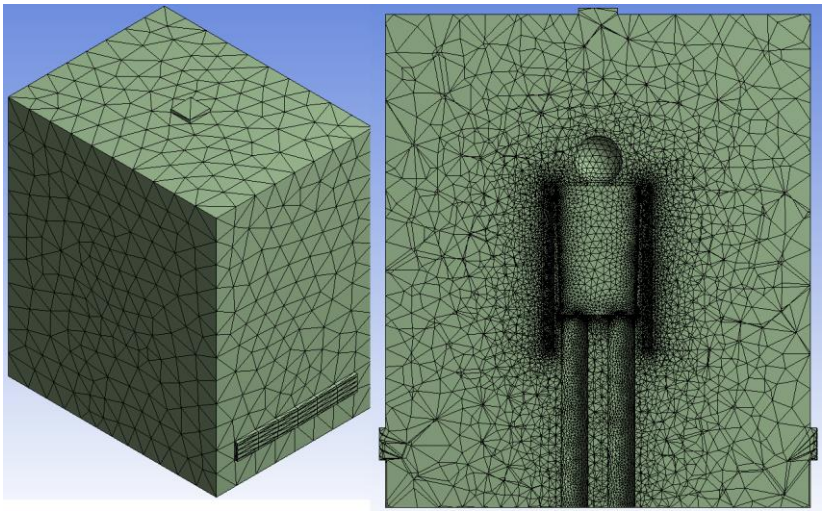

Fig. 4. Meshed fluid volume (left) and sectioned front view (right)

2.2 Simulation Setup

ASHRAE Standard 55 recommended the optimal air temperature and air velocity are 20 °C to 22 °C (this temperature range will be used as benchmark in this study) and less than 0.8 m/s (for under low and sedentary activity levels) [14]. Relative humidity is a controllable factor in thermal comfort, but most studies do not consider it as the fluctuation of humidity levels only result in the perceived temperature difference of 1 °C to 2 °C [15].

Upon successful meshing of the geometric models, simulation setups are then carried out on a 4-core processor and 8GB RAM computer. The simulations are conducted under transient state conditions and a gravitational acceleration of 9.81 ms^{-2} in the negative-y direction. A realizable k-epsilon turbulence model is selected for the simulations to provide accurate results of the turbulent airflow. The model is based on two transport equations, Eq. (1) and (2) given by [16]:

$$\frac{\partial}{\partial t}(\rho k)+\frac{\partial}{\partial x_{\mathrm{i}}}(\rho k u_{\mathrm{i}})=\frac{\partial}{\partial x_{\mathrm{j}}}\left\{\left[\mu+\frac{\rho C_{\mu} k^{2}(\varepsilon)^{-1}}{\sigma_{\mathrm{k}}}\right]\right\}+G_{\mathrm{k}}+G_{\mathrm{b}}-\rho\varepsilon-Y_{\mathrm{M}}+S_{\mathrm{k}} \quad (1)$$

$$\frac{\partial}{\partial t}(\rho \varepsilon)+\frac{\partial}{\partial x_{\mathrm{i}}}(\rho \varepsilon u_{\mathrm{i}})=\frac{\partial}{\partial x_{\mathrm{j}}}\left\{\left[\mu+\frac{\rho C_{\mu} k^{2}(\varepsilon)^{-1}}{\sigma_{\varepsilon}}\right]\frac{\partial \varepsilon}{\partial x_{\mathrm{j}}}\right\}+C_{1\varepsilon}\frac{\varepsilon}{k}(G_{\mathrm{k}}+C_{3\varepsilon}G_{\mathrm{b}})-C_{2\varepsilon}\rho\frac{\varepsilon^{2}}{k}+S_{\varepsilon} \quad (2)$$

where $C_{1\varepsilon}$ = 1.44, $C_{2\varepsilon}$ = 1.92, C_{μ} = 0.09, σ_k = 1.0, σ_ε = 1.3, G_k = generation of turbulence kinetic energy due to the mean velocity gradients, G_b = generation of turbulence kinetic energy due to buoyancy, Y_M = contribution of the fluctuating dilatation in compressible turbulence to the overall dissipation rate S_k and S_ε are user-defined source terms, where in this study both terms are set to zero [16]. As for the radiation model, the Discrete Ordinates (DO) model is selected for its high accuracy and comprehensiveness, which accounts for radiative absorption, emission, and scattering. By default, ANSYS Fluent assigns air as the fluid material and aluminum as the solid material. A third solid material was required for this simulation, which was human skin. The material's characteristics such as density, heat transfer coefficient, temperature, and heat generation rate were determined and assigned to the human model so that the heat transfer simulations can be performed accurately.

The exhaust fan geometry is simplified and did not contain proper moving parts such as the impeller and backdraft damper. Thus, the specifications of the fan are assigned to the simulation based on its specifications table in TCF's study [13]. To simulate for comfort level, the intake fan for the conventional system will operate at 35 Pascal gauge. The exhaust fan operates at a maximum of 80 cubic foot per hour at 95 Pascal gauge, but to ensure similar operating properties, the exhaust fan will operate at 35 Pascal gauge also. The dynamic air vents' boundary conditions were assigned as 'inlet vents' to allow airflow into the passenger lift and to analyse the air velocities and temperatures entering the lift car. Conversely, the ventilation holes' boundary conditions were assigned as 'outlet vents' to allow airflow out of the passenger lift into the lift shaft. The temperature of the fluid volume and human model are assigned last prior to simulation. The fluid volume has an initial temperature of 21 °C, whereas the human model has a skin temperature of 33 °C. A time-step size of 0.01 second is assigned for every simulation to obtain accurate data and results. Time-step sizes of less than 0.01 seconds are possible to obtain more accurate results but will lead to long computational times. A maximum number of time-steps of 2,000 will result in 20 seconds of simulation for both conventional and alternative systems. Twenty iterations per time-step is assigned to allow the simulation to perform 20 sets of calculations per 0.01 second. Thus, 40,000 sets of calculations are performed per simulation.

Prior to running the calculations, solution reports are defined to allow the calculation to provide the simulations' necessary data in the form of texts and graphs. The form of visual results eases the comparison of data between the conventional and alternative designs. These include the volume flow rates, velocities, temperatures, and pressures at the inlets, outlets, and just around the human model.

3. Results

The section presents the results and discussion for airflow and heat transfer analysis for alternative and conventional ventilation systems.

3.1 Grid Independence Study

As one set of results cannot ensure that the simulation is run properly and accurately, a grid independence study is carried out to observe the results for different grid sizes. Grids of 200,000, 300,000, 400,00, and 500,000 tetrahedral cells are used for the airflow analysis to determine the

maximum air velocity at the dynamic air vents inside a non-moving lift car. To generate different grids, the cell size inside the lift car is varied, but other areas such as the walls, vents, and human model are kept constant. First and second order discretisation schemes are used to compare the air velocities between each mesh models. Maximum velocities inside the lift car only varied slightly for grids between 400,000 and 500,000 cells shown in Table 1. Thus, a grid size of no less than 450,000 cells is selected for all airflow and heat transfer analysis.

Table 1
Maximum velocities at dynamic air vents under differing grid sizes

Grid Size	Velocities at Dynamic Air Vents (m/s)			
	200,000 cells	300,000 cells	400,000 cells	500,000 cells
First Order	0.3397	0.3354	0.3317	0.3427
Second Order	1.0412	0.3481	0.3394	0.3520
Difference (%)	67.37	3.65	2.27	2.64

3.2 Airflow Analysis for Alternative Ventilation System

Airflow analysis of both conventional and alternative ventilation systems are carried out and compared. For the alternative design, multiple analysis is carried out for dynamic air vents at different damper angles to determine the optimal angle. The dampers are simulated from 0° to 80° in both rotational directions at an increment of 10°. 17 sets of velocities are obtained and compared in Table 2. From 10° to 80°, the dampers are rotated in the counter-clockwise direction when the lift car travels upwards. Conversely, the dampers are rotated in the clockwise direction between angles negative 10° and negative 80° when the lift car travels downwards.

Table 2
Velocities at dynamic air vents under differing damper angles

Damper Angles (°)	Velocities at Dynamic Air Vents (m/s)		
	Air Vent 1 (Right Wall)	Air Vent 2 (Rear Wall)	Air Vent 3 (Left Wall)
80	0.32553	0.31247	0.32637
70	0.40280	0.41885	0.39787
60	0.47500	0.43631	0.48058
50	0.49635	0.51374	0.48529
40	0.44070	0.39876	0.44030
30	0.45479	0.39508	0.39236
20	0.39350	0.35367	0.40355
10	0.35015	0.32786	0.34115
0	0.35861	0.33157	0.36132
-10	0.36241	0.34199	0.32398
-20	0.28848	0.43654	0.30553
-30	0.50977	0.57582	0.51867
-40	0.35983	0.34426	0.35498
-50	0.46962	0.44930	0.46329
-60	0.35661	0.34287	0.35916
-70	0.29634	0.30148	0.29234
-80	0.22964	0.23504	0.21986

Air velocities entering the lift car from the dynamic air vents did not exceed 0.8 m/s, which indicates that the design and operating conditions satisfy the thermal comfort requirement in

ASHRAE Standard 55. Based on Table 1, the optimal damper angles are 50° and -30°, where air velocities entering the lift car are the greatest. Airflow velocity dropped drastically when the damper angles exceeded 50° in both directions, due to the dampers nearing the 'closed' position that prohibits flow of air into the passenger lift. Conversely, airflow velocity is considerably low between 20° and -20° as the dampers are fully opened and not effectively diverting airflow into the passenger lift. Figure 5 shows the airflow at the desired damper angles (50° and -30°) just in front of the human model. The airflow is well-distributed within the fluid volume of the passenger lift and the air velocities are average with areas of higher air velocity at the top and bottom of the lift car indicated by the light blue streamline arrows.

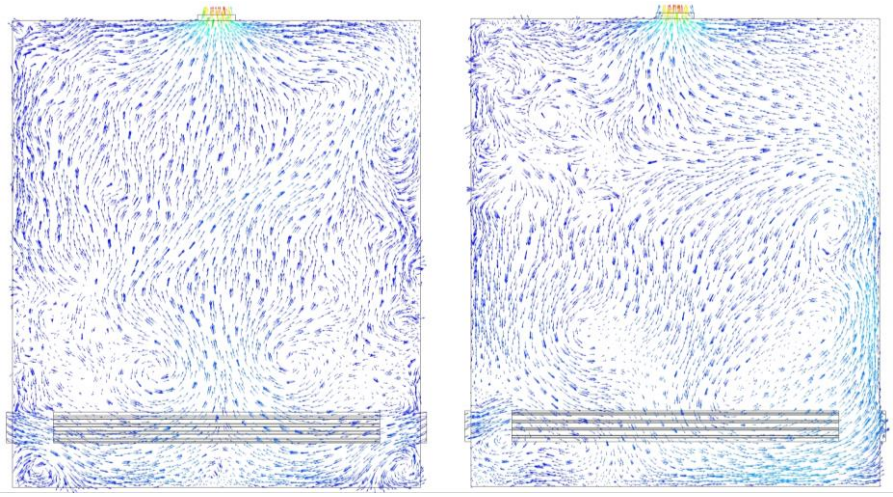

Fig. 5. Airflow analysis of alternative design at 50° (left; while travelling upwards) and -30° (right; while travelling downwards)

3.3 Airflow Analysis for Conventional System

Airflow analysis of the conventional ventilation system is conducted and the average air velocities at the ventilation holes are 5.38 m/s. This result is mainly due to a particular drawback of ANSYS Fluent, which is water-tightness. Geometric models are required to be watertight before meshing can proceed, which in the simulations are the walls of the lift car. However, lift car walls are built in panels, which meant that gaps are present between the panels and car doors to allow air to flow out of the passenger lift. In addition, the total surface area of the ventilation holes is lower as compared to that of the dynamic vents. As both the intake fan and exhaust fan operate under similar conditions, the smaller outlet area of the ventilation holes, on top of the model's water-tightness, would lead to high outlet velocities. Further analysis of the airflow within the fluid volume of the passenger lift showed that the centre of the passenger lift experiences velocities as high as 2 m/s, whereas the surrounding regions are between 0.3 m/s and 0.5 m/s, as shown in Figure 6. Due to the high air velocity and low outlet cross-sectional area, most of the airflow circulated back to the top of the lift rather than being expelled through the ventilation holes. This will cause heat to circulate within the lift instead of effectively expelling through the ventilation holes, which will be determined through the heat transfer analysis.

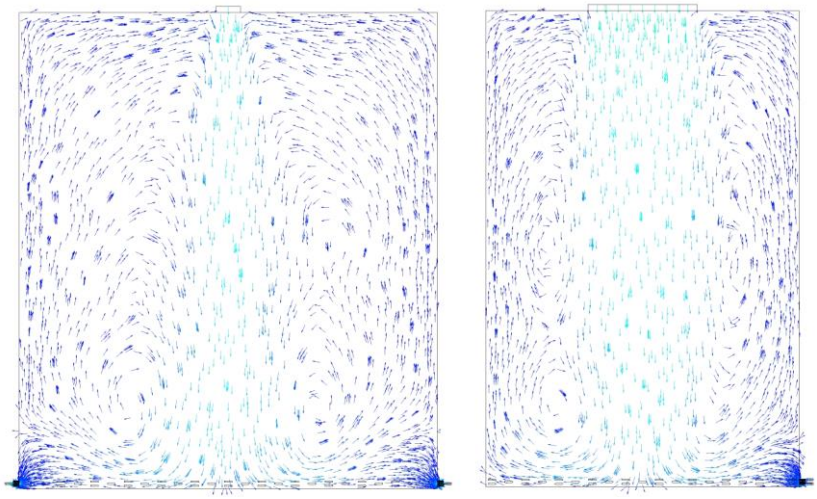

Fig. 6. Airflow analysis of the conventional design as seen from the front (left) and side (right) while travelling upwards

Airflow analysis of both systems are conducted, which showed that the alternative ventilation system is more effective in providing an average airflow velocity throughout the volume of the passenger lift, as compared to the conventional ventilation system. In addition, airflow velocities within the passenger lift with alternative ventilation system did not exceed 0.8m/s, as determined by ASHRAE's standard for thermal comfort.

3.4 Heat Transfer Analysis for Conventional Ventilation System

Heat transfer analysis of both systems are performed, and the simulations are calculated until the solutions reached convergence, which are within 30 seconds of simulation or 3,000 time-steps. A case (.cas) file is written for every five time-steps (0.05 seconds) to animate the airflow and heat transfer from start to finish. The animations are easier to analyse as they showed the entire simulation process, as compared to images of the simulation at convergence. However, computational time was much longer as the case files are needed to be written. The heat transfer analysis of the conventional ventilation system is shown in Figure 7 below.

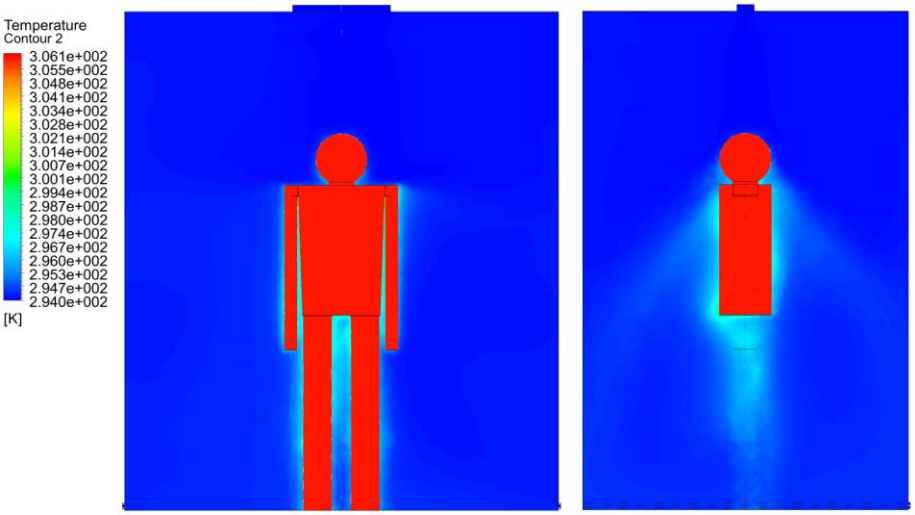

Fig.7. Heat transfer analysis of conventional ventilation system at convergence while travelling upwards: Front view (Left), Side view (Right)

Heat generated by the human model is easily dissipated as it is situated right under the intake fan and thus directly exposed to the 2 m/s wind determined from the airflow analysis. Due to the turbulence created by the intake fan, airflow entering the passenger lift experienced a slight increase in temperature from 21 °C to 22 °C. As a result, the head region was effectively cooled and maintained at 22 °C, provided the passenger remains in the centre of the lift. Heat is effectively transferred away from the upper body area towards the bottom of the passenger lift also, as Figure 7 showed that the air temperature just around the chest area is 24 °C. As for the temperature around the lower body, analysis showed that it maintained at 25 °C for the duration of the simulation as most of the heat generated by the human model is forced to the floor and expelled through the ventilation holes. The simulation achieved convergence in 20 seconds, where at the end of the simulation the entire fluid volume of the lift has increased to about 22 °C. This is mainly caused by the ineffectiveness of the ventilation holes in properly ventilating the heat generated by the human model out of the lift. As some of the heat circulated within the lift, the overall interior temperature increased.

3.5 Heat transfer analysis for alternative ventilation system

For the alternative ventilation system, air is brought in from the dynamic vents and then expelled out from the exhaust fan. Based on the airflow analysis, this design is shown to be more effective in generating average air velocities within the passenger lift. This infers that the passenger would still experience cooling effects from the air by standing at any location within the lift. The simulation results of the alternative ventilation system are shown in Figure 8.

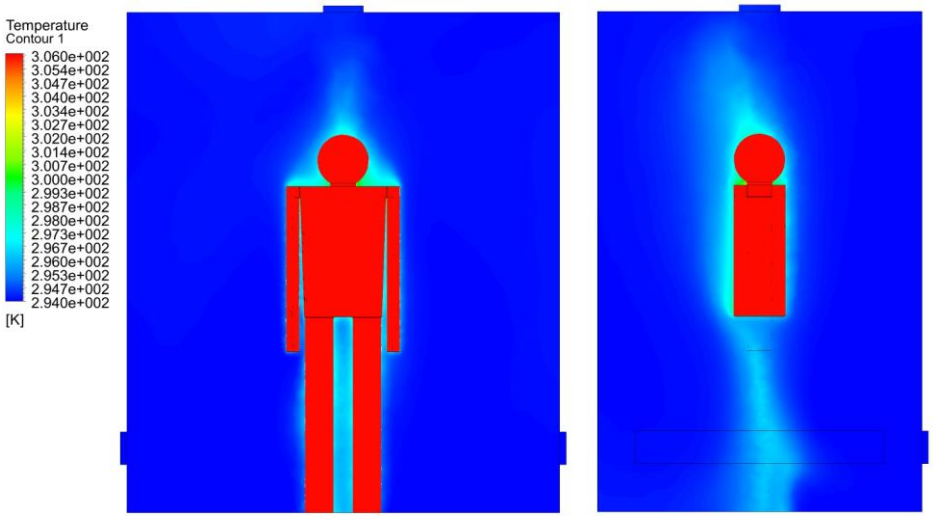

Fig.8. Heat transfer analysis of alternative ventilation system at convergence while travelling upwards: Front view (Left), Side view (Right)

As heat naturally rises due to buoyancy effect, it is easily transferred away from the human model and to the top of the lift car. This is more efficient compared to the conventional ventilation system where heat is transferred to the floor of the lift. As airflow enters through the lower sides of the passenger lift, the lower body of the model is the first section exposed to the moving air. As shown in Figure 8, the temperature just around the lower body is 23 °C. The airflow continues to move upwards and effectively around the upper body of the model. The heat generated from this section is removed effectively as the temperature just around the chest area is at 24 °C. The air temperature just around the head region is at 25 °C, which is slightly higher than the upper and lower body regions as heat from those sections is brought upwards to the exhaust fan. However, the average

temperature within the passenger lift remained at 21 °C, which is lower than the interior temperature analysed in the conventional ventilation system.

From the conventional ventilation system, the difference in temperature between the head and the lower body regions is 3 °C, which is higher than the temperature difference of 2 °C from the alternative ventilation system. This smaller difference in temperature would be more comfortable for passengers as large temperature differences between the parts of the body can lead to thermal discomfort.

4. Conclusions

In this research, an alternative ventilation system consisting of dynamic air vents and an exhaust fan proposed to improve the thermal comfort of passengers inside a lift. From computational fluid dynamics analysis, it is found that airflow is improved by allowing air to enter through the bottom and exiting through the top of the passenger lift. The dynamic vents have greatly improved the distribution of airflow for passengers within the lift. Airflow analysis showed that airflow velocity entering the passenger lift is maximum when the dampers are at 50° and -30°, respectively. Airflow throughout the interior is an average 0.5 m/s, which complies to the thermal comfort in ASHRAE Standard 55. This showed that the concept of implementing dynamic air vents could effectively promote airflow rates into the passenger lift in both directions of travel. The airflow has helped in effectively expelling heat generated by the passenger and maintained the overall temperature within the interior at about 21 °C. Thermal comfort of passengers is satisfied, as the temperature just around the body is an average 24 °C and temperature difference between the head and lower body is 2 °C.

Acknowledgement

The authors would like to acknowledge the assistance and guidance provided by Swinburne University of Technology Sarawak Campus.

References

[1] Caporale, Robert S. "Space and physical requirements." *The Vertical Transportation Handbook* (2010): 181-231.
[2] Zhang, Yang, Xiaowei Sun, Xuefeng Zhao, and Wensheng Su. "Elevator ride comfort monitoring and evaluation using smartphones." *Mechanical Systems and Signal Processing* 105 (2018): 377-390.
[3] Zhou, You, Kai Wang, and Hongxia Liu. "An Elevator Monitoring System Based On The Internet Of Things." *Procedia computer science* 131 (2018): 541-544.
[4] Kwon, Ohhoon, Eunji Lee, and Hyokyung Bahn. "Sensor-aware elevator scheduling for smart building environments." *Building and Environment* 72 (2014): 332-342.
[5] Ang, Jia Hui, Y. Yusup, Sheikh Ahmad Zaki Shaikh Salim, and Mardiana Idayu Ahmad. "A CFD Study of Flow Around an Elevator Towards Potential Kinetic Energy Harvesting." *Journal of Advanced Research in Fluid Mechanics and Thermal Sciences* 59, no. 1 (2019): 54-65.
[6] So, Albert, Lutfi Al-Sharif, and Ahmad Hammoudeh. "Concept design and derivation of the round trip time for a general two-dimensional elevator traffic system." *Journal of Building Engineering* 5 (2016): 165-177.
[7] Yang, Dong-Ho, Ki-Young Kim, Moon K. Kwak, and Seungjun Lee. "Dynamic modeling and experiments on the coupled vibrations of building and elevator ropes." *Journal of Sound and Vibration* 390 (2017): 164-191.
[8] Kwon, Dong-Jun, Jong-Hyun Kim, Sung-Min Park, Il-Jun Kwon, K. Lawrence DeVries, and Joung-Man Park. "Damage sensing, mechanical and interfacial properties of resins suitable for new CFRP rope for elevator applications." *Composites Part B: Engineering* 157 (2019): 259-265.
[9] Gołuch, Piotr, Janusz Kuchmister, Kazimierz Ćmielewski, and Henryk Bryś. "Multi-sensors measuring system for geodetic monitoring of elevator guide rails." *Measurement* 130 (2018): 18-31.
[10] Limaye, Varad M., M. D. Deshpande, M. Sivapragasam, and Vivek Kumar. "Design of dynamic airvents and airflow analysis in a passenger car cabin." *SASTECH* 11, no. 1 (2012): 41-48.
[11] NASA. Anthropometry and biomechanics, 2018.
[12] Pelonis. Model Number JE-06018A23H, AC Cross Flow Fan JE-060A Series, 2019.

[13] TCF. Twin City Fan ceiling & inline/cabinet ventilatos, 2018.
[14] American Society of Heating, Refrigerating, Air-Conditioning Engineers, and American National Standards Institute. *Thermal environmental conditions for human occupancy*. Vol. 55, no. 2004. American Society of Heating, Refrigerating and Air-Conditioning Engineers, 2004.
[15] Kiseliova, Tatiana, Marina Fandoeva, and Anna Sikharulidze. "Investigation of heat waves with fuzzy methods." *Applied Soft Computing* 19 (2014): 102-111.
[16] ANSYS. Standard k-ε model, 2006.